Title:

Effect of lidocaine on dynamic changes in cortical NADH fluorescence during transient focal cerebral ischemia in rats

Authors:

Hiromichi Naito, M.D.,

Department of Anesthesiology, Okayama University Medical School

Yoshimasa Takeda, M.D., Ph.D.,

Associate Professor, Department of Anesthesiology, Okayama University Medical School

Tetsuya Danura, M.D.,

Department of Anesthesiology, Okayama University Medical School

Ira S Kass, Ph.D.,

Professor, Departments of Anesthesiology and Physiology and Pharmacology,

State University of New York Downstate Medical Center

Kiyoshi Morita, M.D., Ph.D.,

Professor and Chairman, Department of Anesthesiology, Okayama University Medical School

Correspondence to: Y. Takeda, Department of Anesthesiology, Okayama University Medical School, 2-5-1 Shikata-cho, Okayama, Japan; Zip code: 700-8558; E-mail address: yoshit@cc.okayama-u.ac.jp; Telephone number: +81-86-235-7327

Figures, 8; tables, 4

Key words: hypoxia; infarction; lidocaine; NADH fluorescence; DC potential; depolarization

Abstract

Rats were subjected to 90 min of focal ischemia by occluding the left middle cerebral and both common carotid arteries. The dynamic changes in formation of brain ischemic areas were analyzed by measuring the direct current (DC) potential and NADH fluorescence with ultraviolet irradiation. In the lidocaine group (n = 10), 30 min before ischemia, an intravenous bolus (1.5 mg/kg) of lidocaine was administered, followed by a continuous infusion (2 mg/kg/h) for 150 min. In the control group (n = 10), an equivalent amounts of saline was administered. Following the initiation of ischemia, an area of high-intensity NADH fluorescence rapidly developed in the middle cerebral artery territory in both groups and the DC potential in this area showed ischemic depolarization. An increase in NADH fluorescence closely correlated with the DC depolarization. The blood flow in the marginal zone of both groups showed a similar decrease. Five minutes after the onset of ischemia, the area of high-intensity NADH fluorescence was significantly smaller in the lidocaine group (67% of the control; P = 0.01). This was likely due to suppression of ischemic depolarization by blockage of voltage dependent sodium channels with lidocaine. Although lidocaine administration did not attenuate the number of peri-infarct depolarizations during the ischemia, the

high-intensity area and infarct volume were significantly smaller in the lidocaine group both at the end of ischemia (78% of the control; $P = 0.046$) and 24 h later ($P = 0.02$). A logistic regression analysis demonstrated a relationship between the duration of ischemic depolarization and histologic damage and revealed that lidocaine administration did not attenuate neuronal damage when the duration of depolarization was identical. These findings indicate that the mechanism by which lidocaine decreases infarct volume is primarily through a reduction of the brain area undergoing NADH fluorescence increases which closely correlates with depolarization.

1 Introduction

Cerebral infarction is a potential consequence of brain ischemia, which may be induced by neurologic or cardiac surgery. Lidocaine may protect neurons during brain ischemia; a number of studies have suggested that lidocaine has neuroprotective effects. In 2 randomized, double-blinded, prospective clinical studies, continuous administration of lidocaine significantly ameliorated postoperative cognitive dysfunction in patients undergoing cardiac surgery for left heart valve procedures (Mitchell et al., 1999) or coronary artery bypass surgery with cardiopulmonary bypass (Wang et al., 2002). In animal models of ischemia, administration of lidocaine has been shown to ameliorate cognitive dysfunction (Popp et al., 2011) and reduce infarct volume (Shokunbi et al., 1990; Lei et al., 2001, 2004). Sodium entry and loss of membrane potential comprise some of the first steps in the development of ischemic neuronal damage. The primary neuroprotective mechanism of lidocaine may be related to blockade of voltage-dependent sodium channels, which results in suppression of cellular energy requirements (Fried et al., 1995; Raley-Susman et al., 2001; Seyfried et al., 2005) and delayed ischemic depolarization (Ayad et al., 1994; Liu et al., 1997). The mechanism by which lidocaine decreases infarction after focal ischemia is not fully understood but may

be associated with suppression of the size of the area of ischemic depolarization, an attenuation of the peri-infarct depolarizations (PIDs), and/or a reduction of neurologic damage during the ischemic depolarization.

Nicotinamide adenine dinucleotide (NAD^+/NADH) is an electron carrier in the mitochondrial respiratory chain. Under conditions of ischemia, NADH accumulates in mitochondria due to the increase in anaerobic glycolysis and an inhibition of mitochondrial oxidative phosphorylation. NADH fluorescence has been used in the past to identify the redox state of mitochondria (Eng et al., 1989; Takeda et al., 2004) due to the unique behavior of NADH which, when excited with ultraviolet light (366 nm), the reduced form (NADH) fluoresces (460 nm emission), while the oxidized form (NAD^+) does not. Because membrane depolarization is accompanied by an increase in energy demand that leads to accumulation of NADH in mitochondria, dynamic changes on the cortical surface can be visualized by NADH fluorescence (Strong et al., 1996; Higuchi et al., 2002; Sasaki et al., 2009).

The purpose of this study is to elucidate the effect of lidocaine on dynamic changes in areas of ischemic depolarization, the propagation of PIDs, and the relationship between ischemic depolarization and neurologic damage. We used simultaneous NADH fluorescence images and two-point direct current (DC) potential

measurements to provide both temporal and spatial observations during 90 min of focal ischemia.

2 Experimental Procedures

2.1 Animals

All experiments were performed in accordance with the National Institutes of Health Guide for the Care and Use of Laboratory Animals and were approved by the Animal Research Control Committee of Okayama University Medical School. All efforts were made to minimize the number of animals used and their suffering. Twenty-two male Sprague Dawley rats (Charles River Laboratories Japan, Yokahama, Japan), weighing 304 ± 23 g, were used as a model of transient focal ischemia in this study. The animals were deprived of food for 8 h prior to the experiments.

2.2 Experimental groups

Animals were randomly assigned to 2 groups: the lidocaine group (n = 10) and the control group (n = 10). An additional 2 rats were placed in a separate sham operation group. In the lidocaine group, a bolus dose of lidocaine (1.5 mg/kg, at a concentration of 1 mg/mL in saline) was administered intravenously 30 min before the initiation of ischemia. The bolus was followed by a continuous infusion of lidocaine at 2 mg/kg/h, which was continued until 30 min after reperfusion. In the control group, an equivalent

amount of saline was administered as sham treatment.

2.3 General procedures

Anesthesia was induced with a mixture of 4% isoflurane in oxygen. After oral tracheal intubation, anesthesia was maintained by artificial ventilation (SN-480–7, Shinano Manufacturing, Tokyo, Japan) with 2% isoflurane in 40% oxygen balanced with nitrogen. A polyethylene catheter (PE50) was placed in the right femoral artery for continuous mean arterial blood pressure monitoring and blood sampling and another was placed in the right femoral vein for administration of saline or lidocaine. Arterial blood gases were measured (i-STAT 300F, Abbott Point of Care, Princeton, NJ, USA) before the ischemia and maintained within the normal range. After the animal was placed in a stereotaxic apparatus (Narishige, Tokyo, Japan), an incision was made on the scalp. The parietal-temporal bone was exposed and the temporal muscles were partially resected. Then, a large cranial window (12 × 9 mm) was made in the left parietal-temporal bone for the observation of NADH fluorescence. The dura was left in place. To monitor the cortical depolarization associated with the initiation of focal ischemia, 2 borosilicate glass DC electrodes (World Precision Instruments, Sarasota, FL, USA), tip diameter < 5 μm, were placed through dural incisions in the cranial window and lowered to a depth of

750 μm below the cortical surface. The positions of the electrodes were 2 mm posterior to the bregma and 2 mm and 4 mm lateral to the sagittal line, respectively. To measure regional cerebral blood flow (CBF), a laser Doppler flow probe (OmegaFlo FLO-C1, Omegawave, Tokyo, Japan) was placed adjacent to the distal DC electrode. Rectal temperature was monitored and maintained at 37.0 ± 0.5°C using a heated water blanket. Target brain surface temperature was maintained at 37°C in accordance with rectal temperature. To control the brain surface temperature, a gentle flow of warm saline was perfused over the brain surface (Kaplan et al., 1991). Since a pilot study determined that the brain surface temperature was within 1.0 ± 0.5°C below the drip temperature, the drip temperature was measured and maintained at 38.0 ± 0.1°C (brain surface temperature, 37.0 ± 0.5°C).

The surgical preparation for the initiation of focal cerebral ischemia was performed as described by Buchan and colleagues (Buchan et al., 1992). The common carotid arteries (CCAs) were exposed bilaterally and loose ligatures were placed around them. The left middle cerebral artery (MCA) was accessed by piercing the dura inside the cranial window 0–1 mm above the rhinal fissure. Ischemia was initiated by tightening ligatures around the bilateral CCAs and by occluding the left MCA via lifting the vessel to 0–1 mm above the rhinal fissure with an 80-μm stainless-steel hook

attached to a micromanipulator. Reperfusion was initiated after 90 min of focal ischemia. The adequacy of circulation after relief of middle cerebral and common carotid artery occlusion was assessed by direct visual observation with a surgical microscope and by observing the increase in flow with laser Doppler flowmeter. After reperfusion, the removed fragment of the parietal-temporal bone was replaced and all wounds were closed. The rats were extubated and returned to their cages with free access to food and water. Despite partial removal of the parietal-temporal bone, rats were still able to eat and drink. The rats were allowed to survive for 24 h after the onset of ischemia. An additional 2 rats underwent a sham operation in which the hook was placed in contact with a portion of the MCA and removed without lifting the artery.

2.4 Technique for cortical NADH fluorescence imaging

The technique used for cortical NADH fluorescence imaging has previously been described in detail (Hashimoto et al., 2000; Higuchi et al., 2002; Sasaki et al., 2009). Briefly, to excite NADH in the cortical tissues, the cortical surface was illuminated using a 200-W Xenon lamp (Hamamatsu Photonics, Hamamatsu, Japan) equipped with a 365-nm bandpass filter (Asahi Spectra, Tokyo, Japan). Images of NADH fluorescence were obtained using a charge-coupled device camera (ST-9XE, Santa Barbara

Instrument Group, Santa Barbara, CA, USA) with a 460-nm bandpass filter. Images (170 × 170 pixels, width × height) were captured every 15 s. Fluorescence intensity values for each pixel in each NADH fluorescence image were divided by those of the control image obtained before the initiation of focal ischemia and the percent change (80–120%) in NADH fluorescence was expressed in each pixel using a 256 gray-scale.

2.5 Histologic evaluation

Twenty-four hours after the onset of ischemia, all animals were anesthetized with 4% isoflurane. After inserting a cannula into the ascending aorta, each animal was perfused with heparinized physiologic saline (20 units/mL) and 6% paraformaldehyde in 0.1 mol/mL phosphate buffer (pH 7.4). The brain of each animal was removed, embedded in paraffin, and sectioned (5 μm thick) at 1000 μm intervals. To identify the DC recording site, the location was recorded in a photograph in which arteries and veins can be identified for each rat at the time of electrode insertion. The DC recording site was identified after perfusion-fixation and marked using a 27-gauge needle with blue ink on the tip of the needle. The DC recording sites were also sectioned, as described above. All sections were stained with hematoxylin and eosin, examined, and photographed.

Images were analyzed for infarct areas by a researcher blinded to the experimental group. Infarct volumes were calculated by multiplying the infarct area by the slice thickness and integrating over all slices. In addition, at the sites of DC measurement, the number of injured pyramidal neurons in the fifth layer of the parietal-temporal cortex was counted by an observer who was blinded to the study. The percent neuronal damage was calculated as the number of damaged neurons divided by the total number of neurons, in the visual field × 100. Pyramidal neurons showing aggregated chromatin in the nucleus, shrinkage, or eosinophilic staining in the cytoplasm were considered injured.

2.6 Statistical analysis

Experimental data are expressed as mean ± standard deviation (SD). Linear regression models were used to evaluate the correlation between percent changes in NADH fluorescence and the magnitude of negative DC deflection. A probit regression curve was used to evaluate the relationship between neuronal injury and total duration of ischemic depolarization at the site of the DC electrode. A linear regression model was not used to evaluate the correlation since it is likely that the probability of neuronal injury converges to 100% with a very long duration of ischemic depolarization. Instead,

a probit curve, which expresses the probability of occurrence and is generally used to identify the LD_{50} in toxicology, was used. The linear model and the probit curve were drawn using personal-computer software (Origin 8, OriginLab Corporation, Northampton, MA, USA). Parameters obtained from the NADH fluorescence images and the measurements of CBF were analyzed by repeated measures analysis of variance (ANOVA). A Scheffé's F-test was used as a post hoc test if the ANOVA was significant. The physiologic parameters and infarct volumes were compared between the lidocaine and control groups using Student's *t*-test. A P-value < 0.05 was considered significant for all statistical tests.

3 Results

Baseline values of physiologic parameters were measured before the induction of focal ischemia and are shown in Table 1. The values of all parameters were maintained within normal limits throughout the experimental period. There were no significant differences in mean arterial blood pressure, arterial pH, arterial oxygen tension, arterial carbon dioxide tension, hemoglobin, or blood glucose concentration between the control and lidocaine groups.

3.1 Measurements of NADH fluorescence and DC potential

The DC potential was successfully measured at 20 sites in the control group and at 20 sites in the lidocaine group. The DC recording was divided into 2 types according to the pattern of negative DC deflection: (1) peri-infarct depolarization (PID), in which the DC potential showed recurrent depolarization during the 90-min ischemic period and (2) persistent depolarization, in which persistent depolarization of the DC was observed during the 90-min ischemic period. Patterns that initially showed recurrent depolarization, but were eventually replaced by persistent depolarization were categorized as persistent depolarization. The number of DC electrodes that recorded either PIDs or persistent depolarizations is listed in Table 2. Representative traces

illustrating the DC recordings and the intensity of NADH fluorescence in areas adjacent to the distal DC electrode (3 × 3 pixels: 255 × 255 μm^2) are shown in Figure 1. The intensity of NADH fluorescence changed simultaneously with the negative DC deflection and the waveforms of NADH fluorescence were analogous to those of the DC potential. No DC deflection was observed without an accompanying increase in NADH fluorescence and no increase in NADH fluorescence was observed without an accompanying DC deflection. As shown in Figure 2, the peak fluorescence value (percent change from the control) was closely related to the magnitude of negative DC deflection (control: r^2 = 0.89, P < 0.001; lidocaine: r^2 = 0.89, P < 0.001). Due to the similarities in the linear regression relationships between the control and lidocaine groups and the fact that 15 mV magnitude of negative DC deflection corresponded to 120% of the pre-ischemia level of NADH fluorescence, in this study, 80–120% NADH fluorescence was expressed in 256 gray-scales and high-intensity NADH fluorescence was defined as a signal with NADH fluorescence > 120% of the pre-ischemia signal (expressed using a white pixel).

3.2 Dynamic changes in NADH fluorescence

After the initiation of ischemia, the development of high-intensity fluorescence was

observed using a series of NADH fluorescence images. Figure 3 and Figure 4 illustrate the serial changes in NADH fluorescence under ischemic conditions with or without lidocaine. A high-intensity region rapidly developed from the proximal to the distal region of the MCA territory. Five minutes after the initiation of ischemia, the size of these initial high-intensity areas were significantly smaller in the lidocaine group (67% of control) compared to the control group (control: 8083 ± 1917 pixels, 58.4 ± 13.9 mm^2 vs. lidocaine: 5382 ± 2273 pixels, 38.9 ± 16.4 mm^2; $P = 0.01$). As shown in Figure 4, the size of the area with high-intensity fluorescence (>120% pre-ischemia) increased gradually, and then plateaued. Throughout the observation period, the area of high-intensity fluorescence was smaller in the lidocaine group compared to the control group. The size difference between the high-intensity areas in the 2 groups became smaller with time. However, before reperfusion, the area of high-intensity NADH fluorescence was significantly smaller in the lidocaine group, at 78% of the control group (control: 7613 ± 2056 pixels, 55.0 ± 14.9 mm^2 vs. lidocaine: 5904 ± 1456 pixels, 42.7 ± 10.5 mm^2; $P = 0.046$).

Several minutes after the formation of the high-intensity fluorescence area, waves of high-intensity fluorescence (which may correlate with PIDs), with a width of 1–3 mm, were observed at the edges of the high-intensity areas and propagated along

the area. The typical pattern of PID propagation, together with persistent depolarization, is shown in Figure 5. During ischemia, 26 waves were observed in the control group and 23 waves were observed in the lidocaine group. The majority of these waves, in both groups, disappeared without sequelae. However, 7 of 26 waves (26.9%) in the control group and 5 of 23 waves (21.7%) in the lidocaine group did not disappear and eventually enlarged the area of high-intensity NADH fluorescence. The frequencies of these PID-like waves per rat (control: 2.6 ± 1.3 times/rat vs. lidocaine: 2.3 ± 1.4 times/rat; $P = 0.60$) and the appearance of the first (control: 10.8 ± 2.8 min vs. lidocaine: 10.8 ± 4.1 min; $P = 0.96$) and second (control: 28.2 ± 17.7 min vs. lidocaine: 33.1 ± 11.9 min; $P = 0.55$) PID-like waves were not significantly different between the 2 groups.

The present and previous studies (Higuchi et al., 2002; Sasaki et al., 2009) have shown that the majority of the high-intensity NADH fluorescence area forms in approximately 5 min, and that PID-like waves then propagate around the high-intensity area and occasionally enlarge it. Therefore, in this study, we defined the ischemic core as the area of high-intensity NADH fluorescence that forms in 5 min and then gradually enlarges with PID-like waves, and the penumbra (potentially salvageable area) as the distal area external to the high-intensity NADH fluorescence area into which the PID-like waves propagate.

3.3 Measurements of the cerebral blood flow

The CBF in the marginal zone was measured using a laser Doppler flowmeter placed adjacent to the distal DC electrode. As shown in Table 2, at this location, 50% of the cases in the control group showed PIDs (site at penumbra) and 50% showed persistent depolarization (site at ischemic core). CBF was successfully measured at 10 sites in the control group and at 9 sites in the lidocaine group. As shown in Figure 6, immediate reduction of CBF was observed after the onset of ischemia. CBF remained approximately stable for the duration of the 90-min ischemic period. There were no significant differences between the 2 groups during the experiment ($P = 0.97$). CBF was not affected by the propagation of waves of NADH fluorescence.

3.4 Histologic outcome at the DC recording sites

Figure 7 illustrates the close relationship between the total depolarization time during the 90-min ischemic period and the percent of damaged pyramidal neurons in the fifth layer of the parietal-temporal cortex at the DC recording site, as determined by a probit logistic regression curve (control: $r^2 = 0.97$, $P < 0.001$; lidocaine: $r^2 = 0.97$, $P < 0.001$). The P_{50}, the total duration of depolarization that induced ischemic cell changes in 50% of the

pyramidal neurons, was estimated (along with corresponding 95% confidence intervals) to be 19.8 min (15.9–25.0 min) in the control group and 20.4 min (17.4–23.4 min) in the lidocaine group. The 95% confidence intervals in both groups overlapped from end-to-end, indicating that there was no significant difference between the 2 groups in the duration of depolarization necessary to cause identical neuronal damage.

3.5 Infarct size

As shown in Figure 8, the infarct volume 24 h after the onset of ischemia in the lidocaine group was significantly smaller than that in the control group (control: 122.9 ± 31.0 mm^3 vs. lidocaine: 90.4 ± 26.9 mm^3, $P = 0.02$)

In the 2 rats that underwent sham operations, no changes were observed in NADH fluorescence, DC potential, and CBF during the observation period. Almost no neuronal damage was detected by microscopic observation 24 h after the sham operation.

4 Discussion

Lidocaine, which is well known as a sodium channel-blockade, has been widely used as a local anesthetic and antiarrhythmic agent. Numerous laboratory studies have suggested that lidocaine can reduce ischemic neuronal injury. As shown in Table 3, administration of lidocaine ameliorates the electrophysiological activities and reduces infarct volume during focal ischemia. Lei et al. (2001) reported that continuous administration of lidocaine at a clinical dose reduced cerebral infarct size at 48 h and 7 days after MCA occlusion, improved neurologic outcome, and inhibited post-ischemic weight loss in rats. As shown in Table 4, administration of lidocaine has been reported to delay the onset of depolarization (Ayad et al., 1994; Liu et al., 1997; Raley-Susman et al., 2001; Seyfried et al., 2005), reduce the amplitude of negative DC deflection (Ayad et al., 1994; Raley-Susman et al., 2001), and facilitate the recovery of membrane potential from depolarization (Weber and Taylor, 1994; Niiyama et al., 2005). Primary neuroprotective mechanism of lidocaine may be related to blockade of voltage-dependent sodium channels, which results in suppression of cellular energy requirements and suppression of ischemic depolarization. However, the mechanism by which lidocaine reduces infarction after transient focal ischemia has not been elucidated. The results of this study suggest that the most likely mechanism underlying

infarct reduction is a reduction of the area of persistent depolarization.

In this study, a 1.5 mg/kg bolus dose of lidocaine was administered 30 min prior to induction of ischemia and lidocaine administration continued at a rate of 2 mg/kg/h. Lei et al. (2001), administered the same dose of lidocaine and reported plasma lidocaine concentrations of 1.2 ± 0.4 μg/mL, 75 min after beginning lidocaine administration. Although plasma concentrations of lidocaine were not measured in the current study, the lidocaine dose and animals used in the current study were identical to those used in the previous report (Lei et al., 2001). Therefore, the plasma concentration of lidocaine was assumed to be similar to these previously reported concentrations. Clinically, the effective plasma lidocaine concentration has been reported as 1.5 μg/mL, when used for antiarrhythmic purposes (Jewitt et al., 1968; Grossman et al., 1969) and it is known that serum concentrations > 5 μg/mL can be toxic (Roden, 2006). Therefore, the dose used in this study represents an antiarrhythmic dose or smaller and is a dose that would be feasible for clinical administration.

In both the control and lidocaine groups, the intensity of NADH fluorescence was closely related to the magnitude of DC deflection, as illustrated by the overlap in 95% confidence intervals for the linear regressions (Figure 2). During depolarization, since the increase in cellular energy demand necessary for restoration of ion

homeostasis is closely associated with the magnitude of DC deflection (Lipton, 1999), large DC deflections may reflect increased glycolysis and result in the increased intensity of NADH fluorescence. Furthermore, Strong et al. (1996), Higuchi et al. (2002), and Sasaki et al. (2009) observed a simultaneous increase in NADH fluorescence and negative DC deflection during ischemic depolarization and propagation of PIDs in animal models. Similarly, Hashimoto et al. (2000) observed a simultaneous increase in NADH fluorescence and negative DC deflection during the propagation of spreading depression in gerbils.

Five minutes after the initiation of ischemia, the size of the area that developed high-intensity NADH fluorescence in the lidocaine group was 67% of the size of the area in the untreated ischemic (control) group. This result suggests that administration of lidocaine improved the balance in mitochondrial energy supply and demand at the periphery of ischemic area. In this study, no significant difference was demonstrated between the 2 groups with respect to the CBF measured in the marginal zone. Using the same lidocaine dose, Lei et al. (2002, 2004) found no significant difference in CBF at either the core or the penumbral areas with administration of lidocaine. Therefore, in the current study, it is assumed that lidocaine decreased energy consumption by suppressing loss of membrane potential with the blockade of voltage-dependent sodium

channels. In support of this notion, Raley-Susman et al. (2001) and Niiyama et al. (2005) administered a 10-μM dose of lidocaine in rat brain slices and found that the loss of membrane potential was suppressed and that the ATP level was preserved at 5 min and 6 min after the induction of ischemia.

PIDs are thought to contribute to infarct expansion because of a positive relationship between infarct volume and the number of PIDs (Iijima et al., 1992; Mies et al., 1993). NADH fluorescence waves, which are highly correlated with the PIDs, were similar in the control and lidocaine groups with respect to the onset time and the number of waves generated. In the penumbra, PIDs are thought to be generated by glutamate and potassium released from the ischemic core (Mies et al., 1994; Dirnagl et al., 1999). Previous studies have reported that administration of lidocaine did not suppress glutamate release at doses < 5 mg/kg (Terada et al., 1999). Since the lidocaine was infused at the rate of 2 mg/kg/h (total dose: 5 mg/kg in 150 min) in this study, glutamate release was not likely to be suppressed. Therefore, the onset time and number of PIDs may not have been affected in the present study.

Since ischemic depolarization is an early step in the ischemic cascade, it is considered one of the most important factors affecting the degree of neuronal damage (Li et al., 2000). From the perspective of ischemic depolarization, neuroprotective

mechanisms can be summarized in 2 categories: (1) to decrease neuronal damage by reducing the area and duration of ischemic depolarization and (2) to decrease neuronal damage by inhibiting the ischemic cascades, triggered by calcium influx following loss of membrane potential during ischemia. In this study, areas of high-intensity NADH fluorescence were decreased with administration of lidocaine. Since the intensity of NADH fluorescence and negative DC deflection were highly correlated, the neuroprotective effect of lidocaine is likely exerted by the first category, reducing the area of NADH fluorescence which corresponds to the area of persistent depolarization.

The relationship between the duration of ischemic depolarization and neuronal damage is shown in Figure 7. Both groups demonstrated a high correlation between these variables (lidocaine: $r^2 = 0.97$, $P < 0.001$; control: $r^2 = 0.97$, $P < 0.001$) and their curves overlap. Furthermore, the total time at which 50% of the neurons show damage (P_{50}) was 20.4 min in the lidocaine group, which is similar to the 19.8-min P_{50} in the control group. These findings indicate that the continuous administration of lidocaine did not affect neuronal damage once persistent depolarization had occurred, likely due to a lack of inhibition of the ischemic cascades.

In conclusion, a continuous infusion of a clinically used antiarrhythmic dose of lidocaine decreased the volume of the cerebral infarct by decreasing the area of the

NADH fluorescence, this correlates with the depolarized ischemic core in which the mitochondrial oxygen demand is increased. Since administration of lidocaine did not attenuate the number of NADH fluorescent PID-like waves during ischemia and did not attenuate neuronal damage when the duration of depolarization was the same, the most likely mechanism underlying infarct reduction is a reduction of the area of persistent depolarization.

References

Ayad M, Verity MA, Rubinstein EH (1994), Lidocaine delays cortical ischemic depolarization: relationship to electrophysiologic recovery and neuropathology. J Neurosurg Anesthesiol 6:98-110.

Buchan AM, Xue D, Slivka A (1992), A new model of temporary focal neocortical ischemia in the rat. Stroke 23:273-279.

Diaz L, Gomez A, Bustos G (1995), Lidocaine reduces the hypoxia-induced release of an excitatory amino acid analog from rat striatal slices in superfusion. Prog Neuropsychopharmacol Biol Psychiatry 19:943-953.

Dirnagl U, Iadecola C, Moskowitz MA (1999), Pathobiology of ischemic stroke: An integrated view. Trends Neurosci 22:391-397.

Dutka AJ, Mink R, McDermott J, Clark JB, Hallenbeck JM (1992), Effect of lidocaine on somatosensory evoked response and cerebral blood flow after canine cerebral air embolism. Stroke 23:1515-1520.

Eng J, Lynch RM, Balaban RS (1989), Nicotinamide adenine dinucleotide fluorescence spectroscopy and imaging of isolated cardiac myocytes. Biophys J 55:621-630.

Evans DE, Catron PW, McDermott JJ, Thomas LB, Kobrine AI, Flynn ET (1989),

Effect of lidocaine after experimental cerebral ischemia induced by air embolism. J Neurosurg 70:97-102.

Evans DE, Kobrine AI, LeGrys DC, Bradley ME, (1984), Protective effect of lidocaine in acute cerebral ischemia induced by air embolism. J Neurosurg 60:257-263.

Fried E, Amorim P, Chambers G, Cottrell JE, Kass IS (1995), The importance of sodium for anoxic transmission damage in rat hippocampal slices: mechanisms of protection by lidocaine. J Physiol 489 (Pt 2):557-565.

Fujitani T, Adachi N, Miyazaki H, Liu K, Nakamura Y, Kataoka K, Arai T (1994), Lidocaine protects hippocampal neurons against ischemicdamage by preventing increase of extracellular excitatory amino acids: a microdialysis study in Mongolian gerbils. Neurosci Lett 179:91-94.

Gelb AW, Steinberg GK, Lam AM, Mnninen PH, Peerless SJ, Rassi-Neto A (1988), The effects of a prophylactic bolus of lidocaine in focal cerebral ischemia. Can J Anesth 35:489-493.

Grossman JI, Cooper JA, Frieden J (1969), Cardiovascular effects of infusion of lidocaine on patients with heart disease. Am J Cardiol 24:191-197.

Hashimoto M, Takeda Y, Sato T, Kawahara H, Nagano O, Hirakawa M (2000), Dynamic changes of NADH fluorescence images and NADH content during spreading

depression in the cerebral cortex of gerbils. Brain Res 872:294-300.

Higuchi T, Takeda Y, Hashimoto M, Nagano O, Hirakawa M (2002), Dynamic changes in cortical NADH fluorescence and direct current potential in rat focal ischemia: relationship between propagation of recurrent depolarization and growth of the ischemic core. J Cereb Blood Flow Metab 22:71-79.

Iijima T, Mies G, Hossmann KA (1992), Repeated negative DC deflections in rat cortex following middle cerebral artery occlusion are abolished by MK-801: effect on volume of ischemic injury. J Cereb Blood Flow Metab 12:727-733.

Jewitt DE, Kishon Y, Thomas M (1968), Lignocaine in the management of arrhythmias after acute myocardial infarction. Lancet 291:266-270.

Kaplan B, Brint S, Tanabe J, Jacewicz M, Wang XJ, Pulsinelli W (1991), Temporal thresholds for neocortical infarction in rats subjected to reversible focal cerebral ischemia. Stroke 22:1032-1039.

Lei B, Cottrell JE, Kass IS (2001), Neuroprotective effect of low-dose lidocaine in a rat model of transient focal cerebral ischemia. Anesthesiology 95:445-451.

Lei B, Popp S, Capuano-Waters C, Cottrell JE, Kass IS (2002), Effects of delayed administration of low-dose lidocaine on transient focal cerebral ischemia in rats. Anesthesiology 97:1534-1540.

Lei B, Popp S, Capuano-Waters C, Cottrell JE, Kass IS (2004) Lidocaine attenuates apoptosis in the ischemic penumbra and reduces infarct size after transient focal cerebral ischemia in rats. Neuroscience 125:691-701.

Li J, Takeda Y, Hirakawa M (2000), Threshold of ischemic depolarization for neuronal injury following four-vessel occlusion in the rat cortex. J Neurosurg Anesthesiol 12:247-254.

Lipton P (1999), Ischemic cell death in brain neurons. Physiol Rev 79:1431-1568.

Liu K, Adachi N, Yanase H, Kataoka K, Arai T (1997), Lidocaine suppresses the anoxic depolarization and reduces the increase in the intracellular Ca2+ concentration in gerbil hippocampal neurons. Anesthesiology 87:1470-1478.

LoPachin RM, Gaughan CL, Lehning EJ, Weber ML, Taylor CP (2001), Effects of ion channel blockade on the distribution of Na, K, Ca and other elements in oxygen-glucose deprived CA1 hippocampal neurons. Neuroscience 103:971-983.

Mies G, Iijima T, Hossmann KA (1993), Correlation between periinfarct DC shifts and ischemic neuronal damage in rat. Neuroreport 4:709-711.

Mies G, Kohno K, Hossmann KA (1994), Prevention of periinfarct direct current shifts with glutamate antagonist NBQX following occlusion of the middle cerebral artery in the rat. J Cereb Blood Flow Metab 14:802-807.

Mitchell SJ, Pellett O, Gorman DF (1999), Cerebral protection by lidocaine during cardiac operations. Ann Thorac Surg 67:1117-1124.

Niiyama S, Tanaka E, Tsuji S, Murai Y, Satani M, Sakamoto H, Takahashi K, Kuroiwa M, Yamada A, Noguchi M, Higashi H (2005), Neuroprotective mechanisms of lidocaine against in vitro ischemic insult of rat hippocampal CA1 pyramidal neurons. Neurosci Res 53:271-278.

Popp SS, Lei B, Kelemen E, Fenton AA, Cottrell JE, Kass IS (2011), Intravenous antiarrhythmic doses of lidocaine increase the survival rate of CA1 neurons and improve cognitive outcome after transient global cerebral ischemia in rats. Neuroscience 192:537-549.

Raley-Susman KM, Kass IS, Cottrell JE, Newman RB, Chambers G, Wang J (2001), Sodium influx blockade and hypoxic damage to CA1 pyramidal neurons in rat hippocampal slices. J Neurophysiol 86:2715-2726.

Rasool N, Faroqui M, Rubinstein EH (1990), Lidocaine accelerates neuroelectrical recovery after incomplete global ischemia in rabbits. Stroke 21:929-935.

Roden DM (2006), Antiarrhythmic drugs In: Goodman and Gilman's the Pharmacological Basis of Therapeutics 11th edition (Brunton LL, Lazo JS, Parker KL, eds), pp 899-932. New York: McGraw-Hill.

Sasaki T, Takeda Y, Taninishi H, Arai M, Shiraishi K, Morita K (2009), Dynamic changes in cortical NADH fluorescence in rat focal ischemia: evaluation of the effects of hypothermia on propagation of peri-infarct depolarization by temporal and spatial analysis. Neurosci Lett 449:61-65.

Seyfried FJ, Adachi N, Arai T (2005), Suppression of energy requirement by lidocaine in the ischemic mouse brain. J Neurosurg Anesthesiol 17:75-81.

Shokunbi MT, Gelb AW, Peerless SJ, Mervart M, Floyd P (1986), An evaluation of the effect of lidocaine in experimental focal cerebral ischemia. Stroke 17:962-966.

Shokunbi MT, Gelb AW, Wu XM, Miller DJ (1990), Continuous lidocaine infusion and focal feline cerebral ischemia. Stroke 21:107-111.

Strong AJ, Harland SP, Meldrum BS, Whittington DJ (1996), The use of in vivo fluorescence image sequences to indicate the occurrence and propagation of transient focal depolarizations in cerebral ischemia. J Cereb Blood Flow Metab 16:367-377.

Takeda Y, Pérez-Pinzón MA, Ginsberg MD, Sick TJ (2004), Mitochondria consume energy and compromise cellular membrane potential by reversing ATP synthetase activity during focal ischemia in rats. J Cereb Blood Flow Metab 24:986-992.

Taylor CP, Burke SP, Weber ML (1995), Hippocampal slices: glutamate overflow and cellular damage from ischemia are reduced by sodium-channel blockade. J Neurosci

Methods 59:121-128.

Terada H, Ohta S, Nishikawa T, Mizunuma T, Iwasaki Y, Masaki Y (1999), The effect of intravenous or subarachnoid lidocaine on glutamate accumulation during transient forebrain ishchemia in rats. Anesth Analg 89:957-961.

Wang D, Wu X, Li J, Xiao F, Liu X, Meng M (2002), The effect of lidocaine on early postoperative cognitive dysfunction after coronary artery bypass surgery. Anesth Analg 95:1134-1141.

Weber ML, Taylor CP (1994), Damage from oxygen and glucose deprivation in hippocampal slices is prevented by tetrodotoxin, lidocaine and phenytoin without blockade of action potentials. Brain Res 664:167-177.

Yamada A, Tanaka E, Niiyama S, Yamamoto S, Hamada M, Higashi H (2004), Protective actions of various local anesthetics against the membrane dysfunction produced by in vitro ischemia in rat hippocampal CA1 neurons. Neurosci Res 50:291-298.

Zhang Y, Lipton P (1999), Cytosolic Ca^{2+} changes during in vitro ischemia in rat hippocampal slices: major roles for glutamate and Na^{+}-dependent Ca^{2+} release from mitochondria. J Neurosci 19:3307-3315.

Figure legends

Figure 1

Representative traces showing cerebral blood flow (CBF), NADH fluorescence in areas adjacent to the distal direct current (DC) electrode (3 × 3 pixels: 255 × 255 μm^2) and the DC potential of the peri-infarct depolarizations (PIDs) and the persistent depolarization. The waveform representing NADH fluorescence was analogous to the changes in DC potential.

Figure 2

Relationships between the percent change in NADH fluorescence and the magnitude of negative direct current (DC) deflection were evaluated using linear regression models. The black line and circles represent the control group and the gray line and triangles represent the lidocaine group. 95% confidence intervals are shown with dotted lines (Control group: $r^2 = 0.89$, $P < 0.001$; Lidocaine group: $r^2 = 0.89$, $P < 0.001$).

Figure 3

(A and B) Sequences of NADH fluorescence images. The dashed lines in (A) and (B) represent the cranial window. For visualization of changes in NADH fluorescence, data for each pixel in each NADH fluorescence image was divided by that of the control image obtained before the initiation of focal ischemia. The percent change in NADH fluorescence (80–120%) was expressed in each pixel with 256 gray-scales. These sequences represent the development of areas of high-intensity NADH fluorescence following the initiation of ischemia with or without lidocaine. (A) Formation of the ischemic core (before ischemia to 10 min following initiation of ischemia). Images captured every 1 min are shown. The first image (left top) was taken prior to initiation of ischemia. The wave of high-intensity NADH fluorescence (shown in white) spreads from the area of the middle cerebral artery occlusion. The high-intensity area forms rapidly after the initiation of ischemia, originating from the parietal cortex and propagating along the ischemic core in the anterior and posterior directions. (B) Images during ischemia (from 10 min following initiation of ischemia to 90 min, the end of ischemia). Areas of high-intensity NADH fluorescence were suppressed during ischemia in the lidocaine group. (C) A schematic drawing of the cranial window. The shaded area represents the large cranial window made on the left parietal-temporal bone. The left

middle cerebral artery was observed and occluded inside the cranial window. DC1 and DC2 represent the locations of direct current recording sites.

Figure 4

Development of areas of high-intensity NADH fluorescence and the frequency distribution of peri-infarct depolarizations (PIDs). The line graph corresponds to the number of pixels with >120% of the pre-ischemic levels of NADH fluorescence (i.e., the high-intensity area). The gray line represents the lidocaine group and the black line represents the control group. Throughout the observation period, the area of high-intensity NADH fluorescence was smaller in the lidocaine group compared to the control group (*$P < 0.05$). The bar graph shows the frequency distribution of PIDs in the control group (black) and the lidocaine group (white).

Figure 5

A typical pattern of the propagation of a peri-infarct depolarization (PID) and persistent depolarization. The percent change in NADH fluorescence (80–120%) was expressed in each pixel using 256 gray-scales. Images (A)–(F) correspond to the times Illustrated with gray lines in the graph (lower panel). Circles (red) in the cranial window represent the locations of the direct current (DC) electrodes and correspond to the DC1 and DC2 recording sites. The graph shows NADH fluorescence in areas adjacent to the distal DC electrode (3 × 3 pixels: 255 × 255 μm^2) and the direct current (DC) potential at each recording site. Waves of high-intensity NADH fluorescence with persistent depolarization (ischemic core), detected by subtracting the neighboring image, are superimposed on the images in green. DC2 is involved in the area that shows persistent depolarization (C)–(F). A PID-like wave, detected by subtracting the neighboring image, is superimposed on the images in blue. At DC1, a PID-like wave propagates around the ischemic core and disappeared without enlarging the area of high-intensity NADH fluorescence (D)–(F).

Figure 6

Changes in cerebral blood flow (CBF) measured by a laser Doppler flowmeter in the marginal zone. The laser Doppler probe was placed adjacent to the distal direct current (DC) electrode. The gray line shows the lidocaine group and the black line represents the control group. There was no significant difference between the 2 groups ($P = 0.97$).

Figure 7

Relationship between the total duration of ischemic depolarization and the percent damaged pyramidal neurons at the direct current (DC) recording sites in the fifth layer of the parietal-temporal cortex. Black lines with circles represent the control group and gray lines with triangles represent the lidocaine group (Control: $r^2 = 0.97$, $P < 0.001$; Lidocaine: $r^2 = 0.97$, $P < 0.001$), while 95% confidence intervals (CI) are shown with corresponding dotted lines. Logistic regression curves showed close relationships between the duration of ischemic depolarization and the percent damaged neurons. The total duration of depolarization causing ischemic cell change in 50% of the pyramidal neurons (P_{50}) in the control and lidocaine groups was estimated to be 19.8 min (95% CI: 15.9–25.0 min) and 20.4 min (95% CI: 17.4–23.4 min), respectively.

Figure 8

Infarct size 24 h after reperfusion in the control and lidocaine groups. Brain sections (5 μm thick) were prepared at 1000-μm intervals and stained with hematoxylin and eosin. Infarct volumes were calculated by multiplying the infarct area by the slice thickness and integrating over all slices. Infarct size in the lidocaine group was significantly smaller (*P= 0.02) compared to the control group.

Table 1. Physiological parameters before the ischemia

	Control (n = 10)	Lidocaine (n = 10)
Body weight (g)	298 ± 19.9	297 ± 22.6
MABP (mmHg)	84.2 ± 7.24	87.0 ± 8.3
Arterial pH	7.44 ± 0.04	7.43 ± 0.03
PaO_2 (mmHg)	151.4 ± 32.1	138.8 ± 29.4
$PaCO_2$ (mmHg)	39.0 ± 2.67	40.1 ± 2.45
Hb (g/dL)	13.9 ± 1.21	14.1 ± 1.04
Glucose (mg/dL)	143.3 ± 31.7	162.7 ± 33.6

Values are expressed as means ± S.D. MABP, mean arterial blood pressure; PaO_2, partial pressure of oxygen (arterial); $PaCO_2$, partial pressure of carbon dioxide (arterial); Hb, hemoglobin

Table 2. Number of DC deflection types in each recording site.

	Persistent depolarization	Peri-infarct depolarization	Not depolarized
Distal electrode (DC1)			
Control (n = 10)	5	5	0
Lidocaine (n = 10)	4	5	1
Proximal electrode (DC2)			
Control (n = 10)	10	0	0
Lidocaine (n = 10)	7	2	1
Total			
Control (n = 20)	15	5	0
Lidocaine (n = 20)	11	7	2

The locations of the direct current (DC) recording sites DC1 and DC2 are shown in Figure 3 (C).

Table 3. Effect of lidocaine during focal ischemia

Year published	Authors	Animal	Ischemia model (duration)	Intravenously administered dose	Evaluation method	Outcome
1984	Evans et al.	Cat	Air embolism	5 mg/kg	SER	Improved
1986	Shokunbi et al.	Cat	MCA occlusion (4h or 6h)	50 mg/kg + 50 mg/kg/h	Histology	Unchanged
1988	Gelb et al.	Cat	MCA occlusion (6h)	5 mg/kg	SER, histology	Partially improved
1989	Evans et al.	Cat	Air embolism	1.5 mg/kg + 3 mg/kg + 1 mg/kg (repeated)	SER	Improved
1990	Shokunbi et al.	Cat	MCA occlusion (3h)	5 mg/kg + 3 mg/kg + 2 mg/kg/h	SER, CBF, histology	Improved
1992	Dutka et al.	Dog	Air embolism	1.5 mg/kg + 1 mg/kg (repeated)	SER, CBF	Improved
2001	Lei et al.	Rat	MCA occlusion (90min)	1.5 mg/kg + 2 mg/kg/h	Histology, neurologic score	Improved
2002	Lei et al.	Rat	MCA occlusion (90min)	1.5 mg/kg + 2 mg/kg/h	CBF, histology, neurologic score	Improved
2004	Lei et al.	Rat	MCA occlusion (90min)	1.5 mg/kg + 2 mg/kg/h	CBF, histology	Improved

SER, somatosensory evoked response; MCA, middle cerebral artery; CBF, cerebral blood flow

Table 4. Neuroprotective mechanisms of lidocaine during brain ischemia

Year published	Authors	Animal (model)	Improved evaluation points
1990	Rasool et al.	Rabbit (global ischemia)	Facilitated the recovery of somatosensory evoked potentials
1994	Ayad et al.	Rabbit (global ischemia)	Delayed the onset ischemic depolarization; reduced the amplitude of negative DC deflection
1994	Fujitani et al.	Gerbil (global ischemia)	Suppressed concentration of extracellular excitatory amino acids (aspartate, glutamate, glycine, taurine)
1994	Weber and Taylor	Rat (hippocampal slices)	Facilitated the recovery of membrane potential from ischemic depolarization
1995	Diaz et al.	Rat (striatal slices)	Suppressed concentration of extracellular D-aspartic acid
1995	Fried et al.	Rat (hippocampal slices)	Facilitated the recovery of evoked population spike; preserved ATP content; reduced Na^+ influx during ischemia
1995	Taylor et al.	Rat (hippocampal slices)	Reduced the percentage of depolarized hippocampal slices; suppressed concentration of extracellular glutamate
1997	Liu et al.	Gerbil (global ischemia)	Delayed the onset of ischemic depolarization; suppressed intracellular Ca^{2+} increase
1999	Terada et al.	Rat (global ischemia)	Suppressed concentration of extracellular glutamate
1999	Zhang and Lipton	Rat (hippocampal slices)	Reduced Na+ influx during ischemia; suppressed intracellular Ca^{2+} increase
2001	Lopachin et al.	Rat (hippocampal slices)	Reduced Na^+ influx during ischemia
2001	Raley-Susman et al.	Rat (hippocampal slices)	Delayed the onset of ischemic depolarization; reduced the amplitude of negative DC deflection; preserved ATP content; reduced Na^+ influx during ischemia

2004	Yamada et al.	Rat (hippocampal slices)	Delayed the onset of ischemic depolarization
2005	Niiyama et al.	Rat (hippocampal slices)	Facilitated the recovery of membrane potential from ischemic depolarization; preserved ATP content
2005	Seyfried et al.	Mouse (global ischemia)	Delayed the onset of ischemic depolarization; preserved ATP content

ATP, adenosine triphosphate; DC, direct current

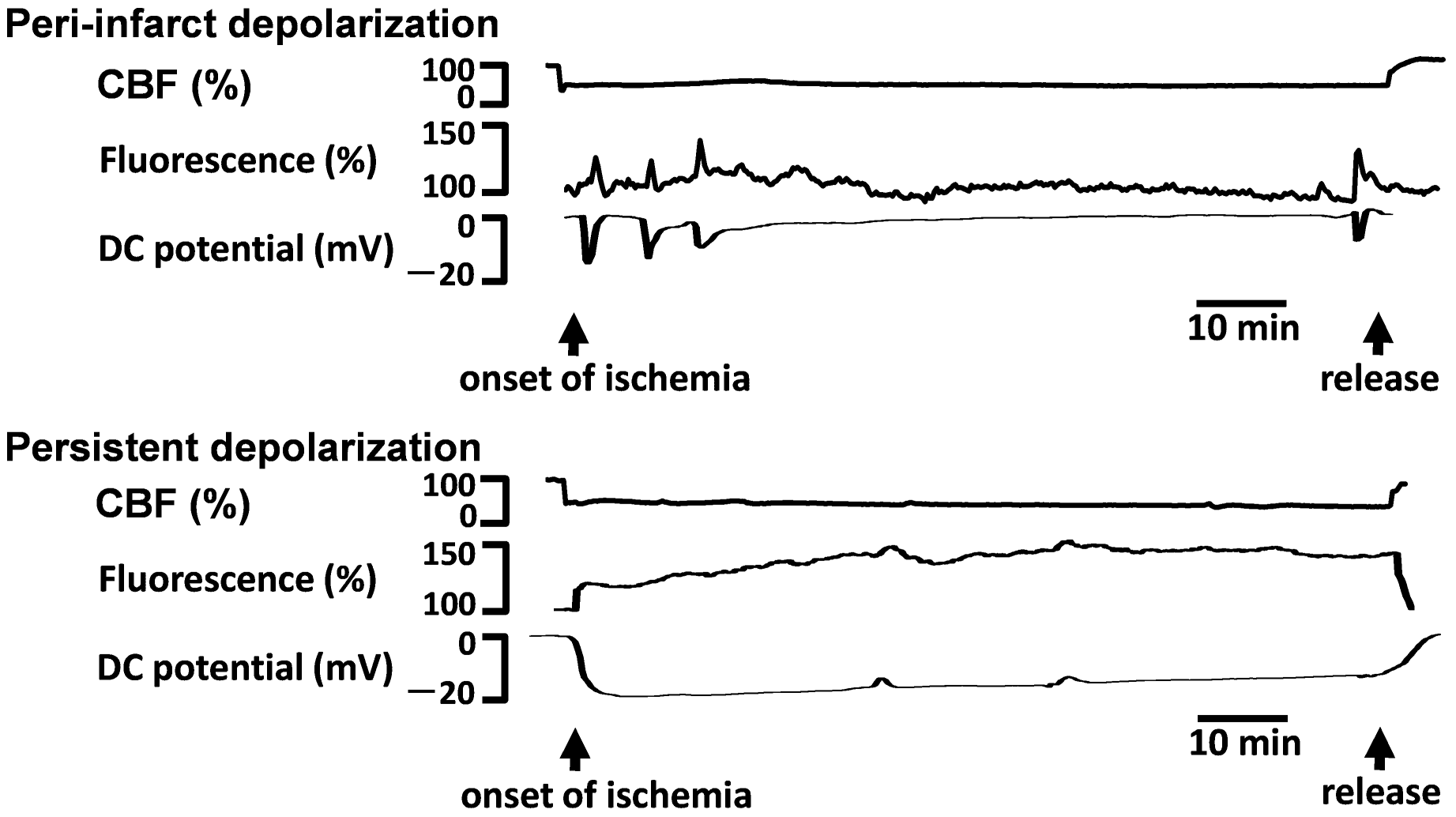
Peri-infarct depolarization
CBF (%)
100
0
Fluorescence (%)
150
100
DC potential (mV)
0
−20
10 min
onset of ischemia
release
Persistent depolarization
CBF (%)
100
0
Fluorescence (%)
150
100
DC potential (mV)
0
−20
10 min
onset of ischemia
release

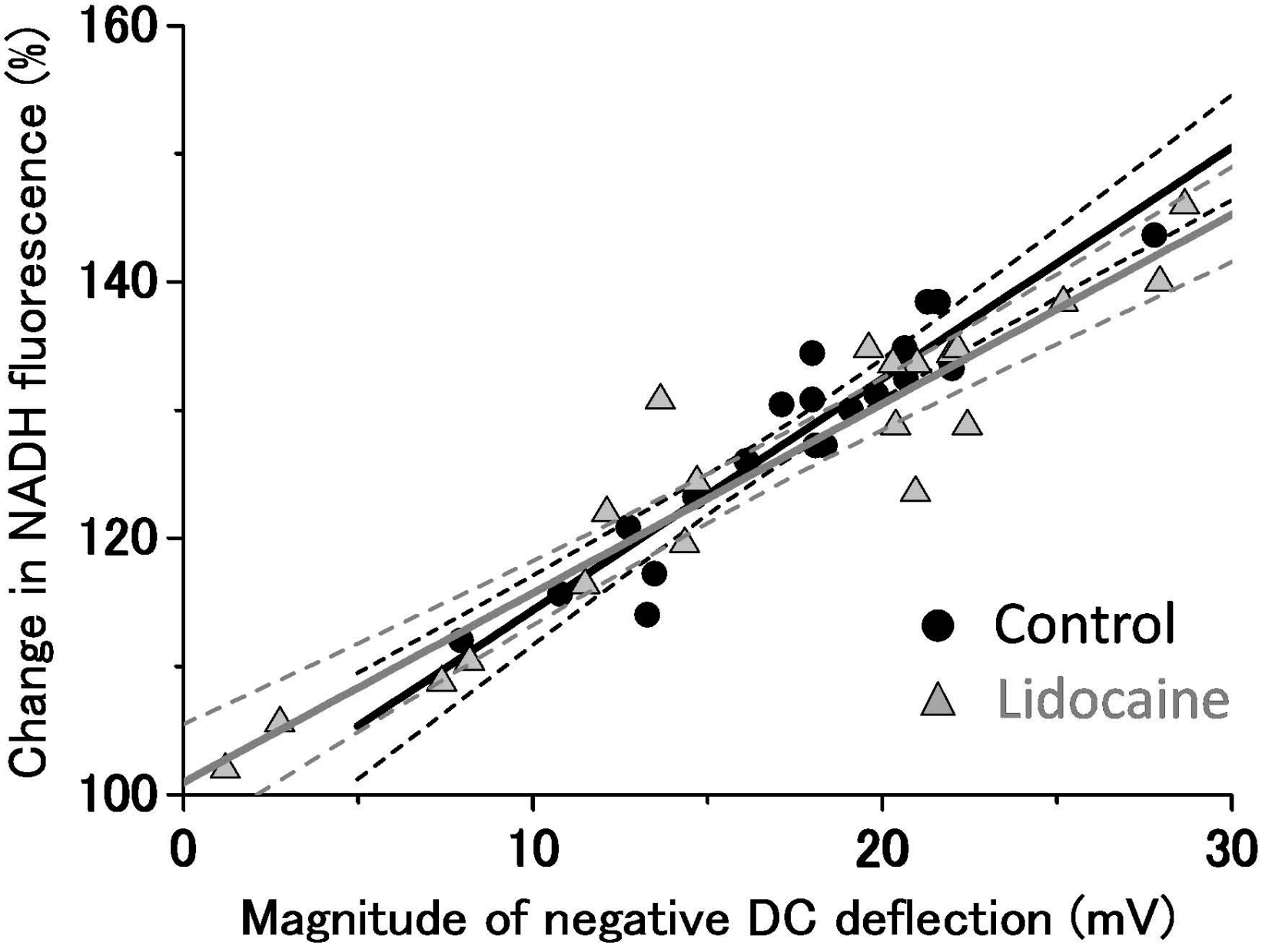
160
140
120
100
0
10
20
30
Change in NADH fluorescence (%)
Magnitude of negative DC deflection (mV)
Control
Lidocaine

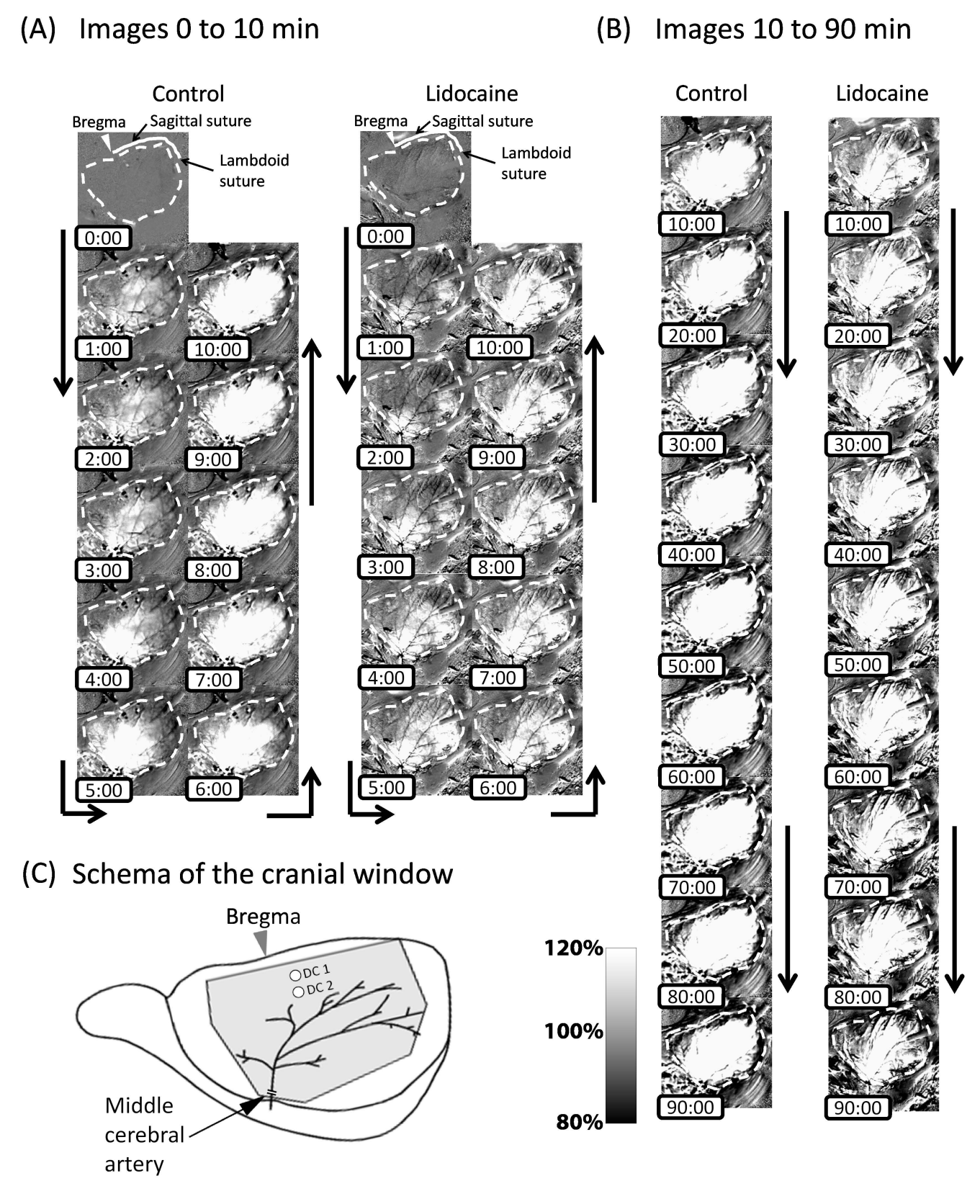
(A) Images 0 to 10 min
(B) Images 10 to 90 min
Control
Lidocaine
Bregma
Sagittal suture
Lambdoid suture
0:00
1:00
2:00
3:00
4:00
5:00
6:00
7:00
8:00
9:00
10:00
20:00
30:00
40:00
50:00
60:00
70:00
80:00
90:00
(C) Schema of the cranial window
DC 1
DC 2
Middle cerebral artery
120%
100%
80%

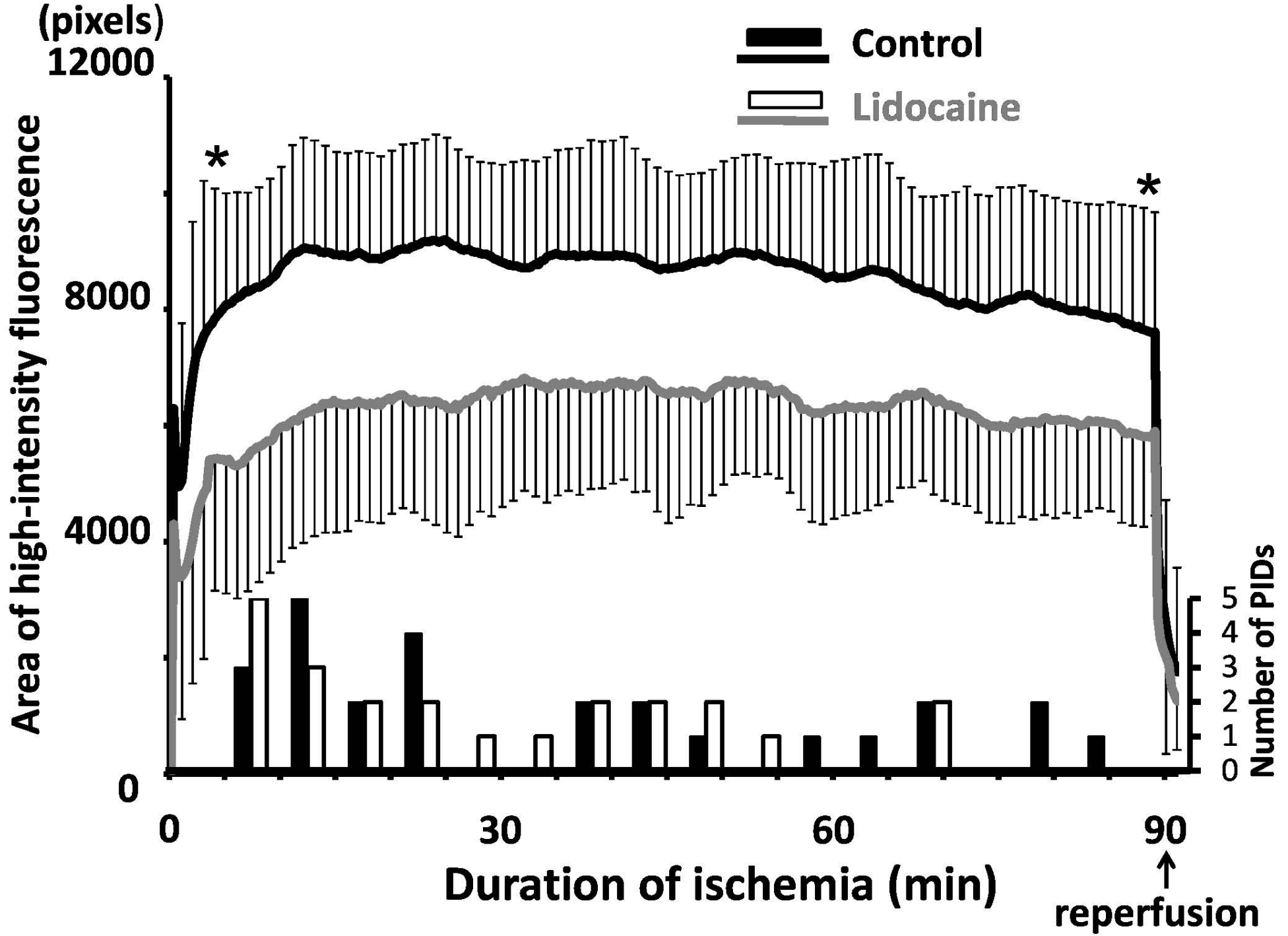
(pixels)
12000
8000
4000
0
Area of high-intensity fluorescence
Control
Lidocaine
*
*
5
4
3
2
1
0
Number of PIDs
0
30
60
90
Duration of ischemia (min)
reperfusion

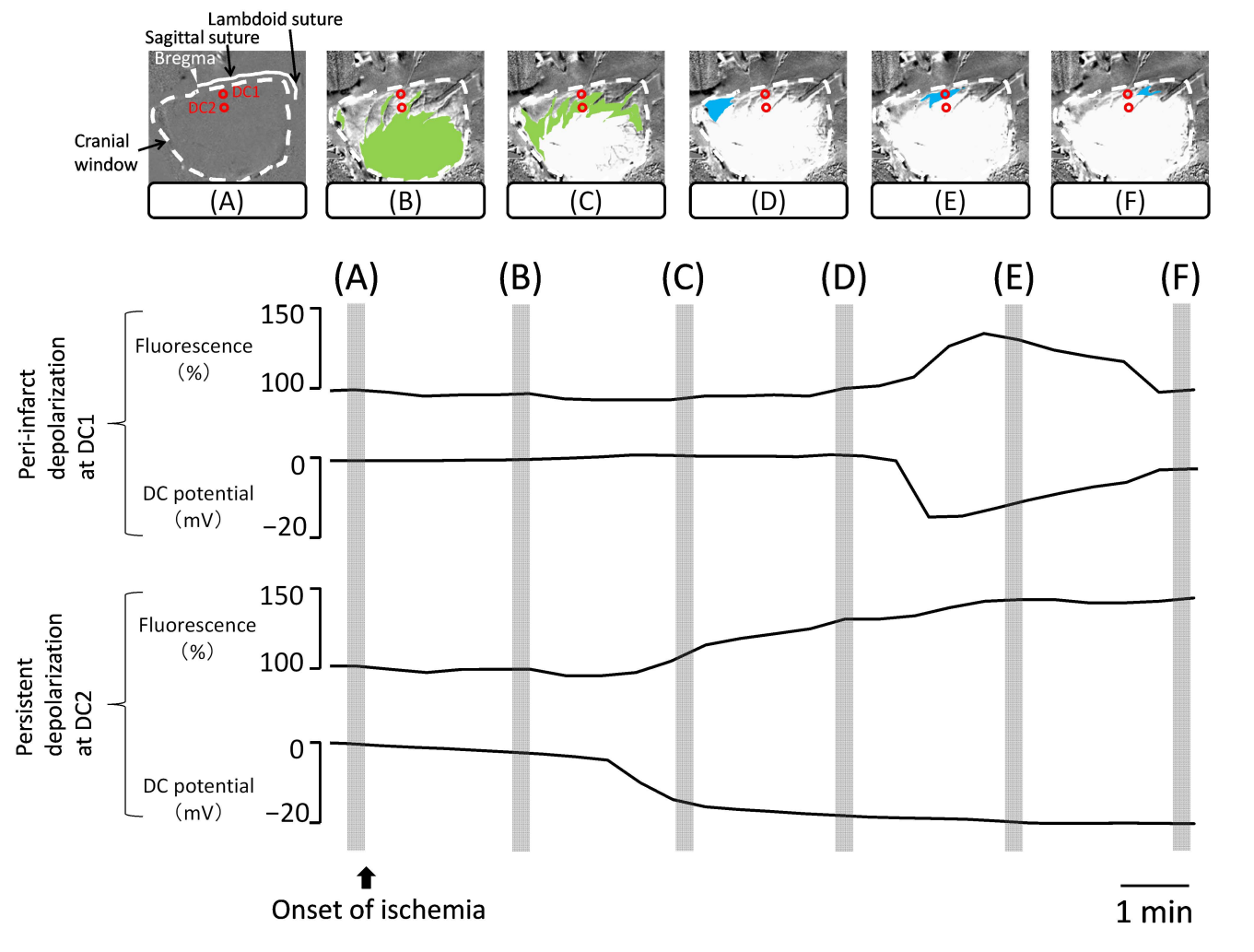
Lambdoid suture
Sagittal suture
Bregma
DC1
DC2
Cranial window
(A)
(B)
(C)
(D)
(E)
(F)
(A)
(B)
(C)
(D)
(E)
(F)
Peri-infarct depolarization at DC1
Fluorescence (%)
150
100
DC potential (mV)
0
−20
Persistent depolarization at DC2
Fluorescence (%)
150
100
DC potential (mV)
0
−20
Onset of ischemia
1 min

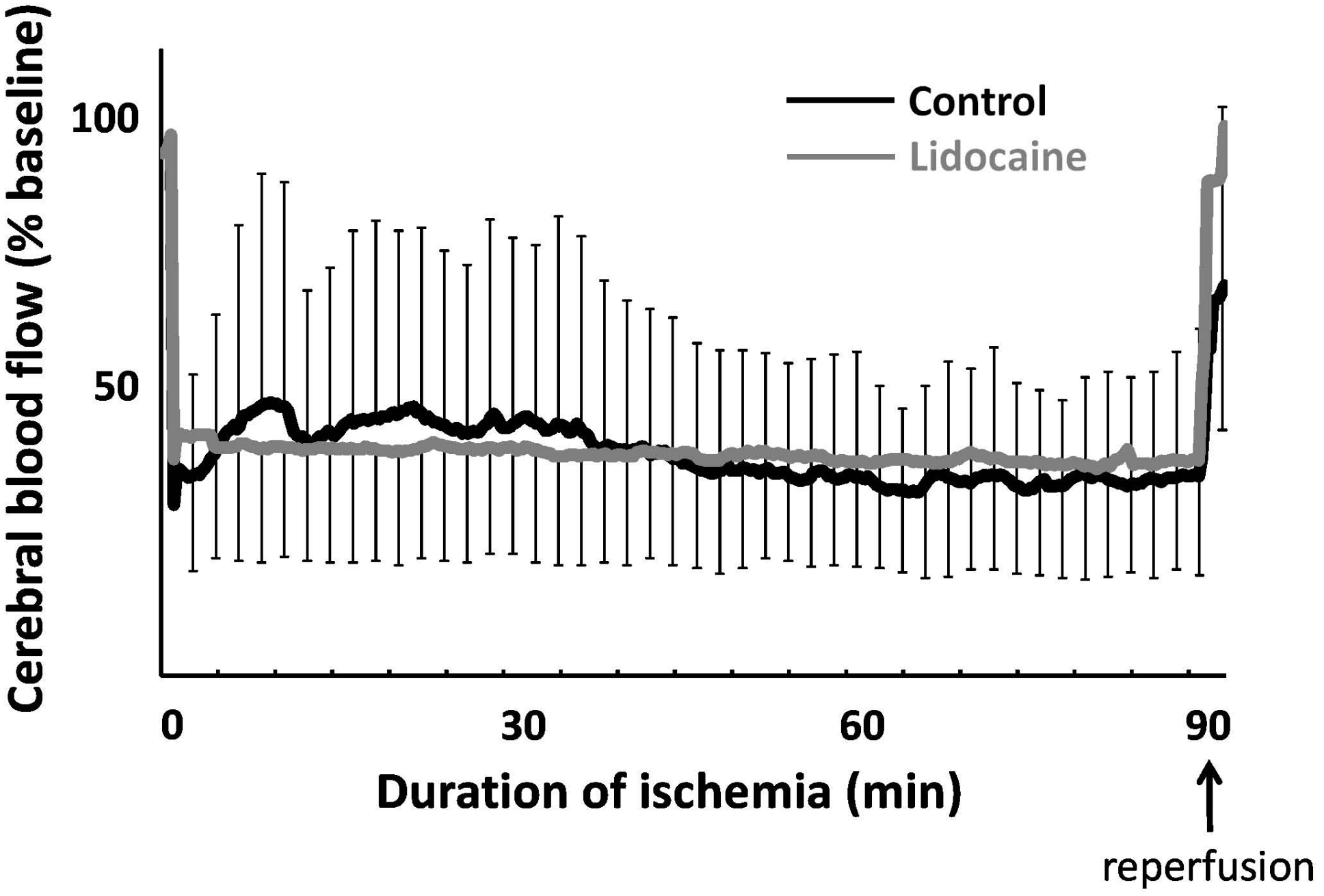
Cerebral blood flow (% baseline)
100
50
Control
Lidocaine
0
30
60
90
Duration of ischemia (min)
reperfusion

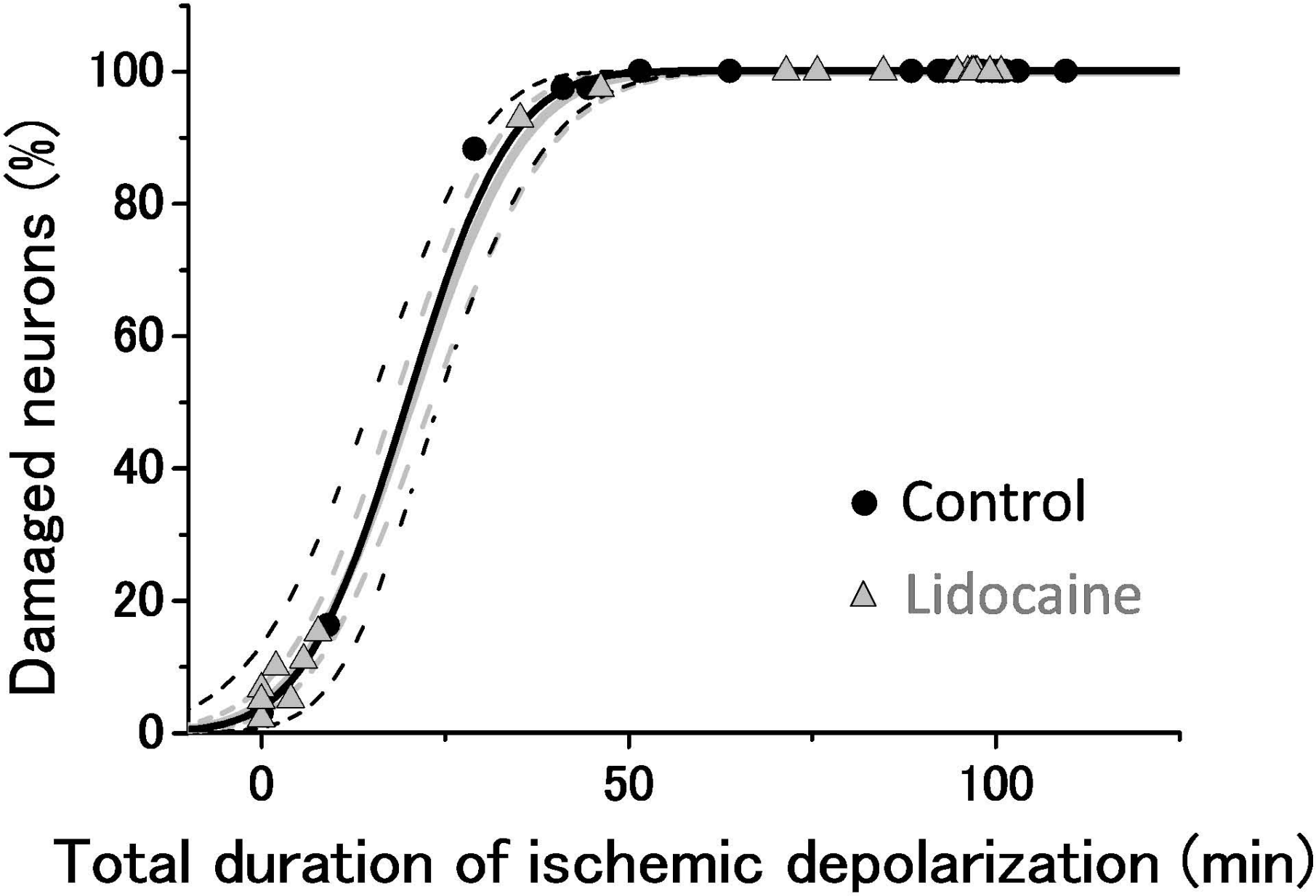
Damaged neurons (%)
100
80
60
40
20
0
0
50
100
Control
Lidocaine
Total duration of ischemic depolarization (min)

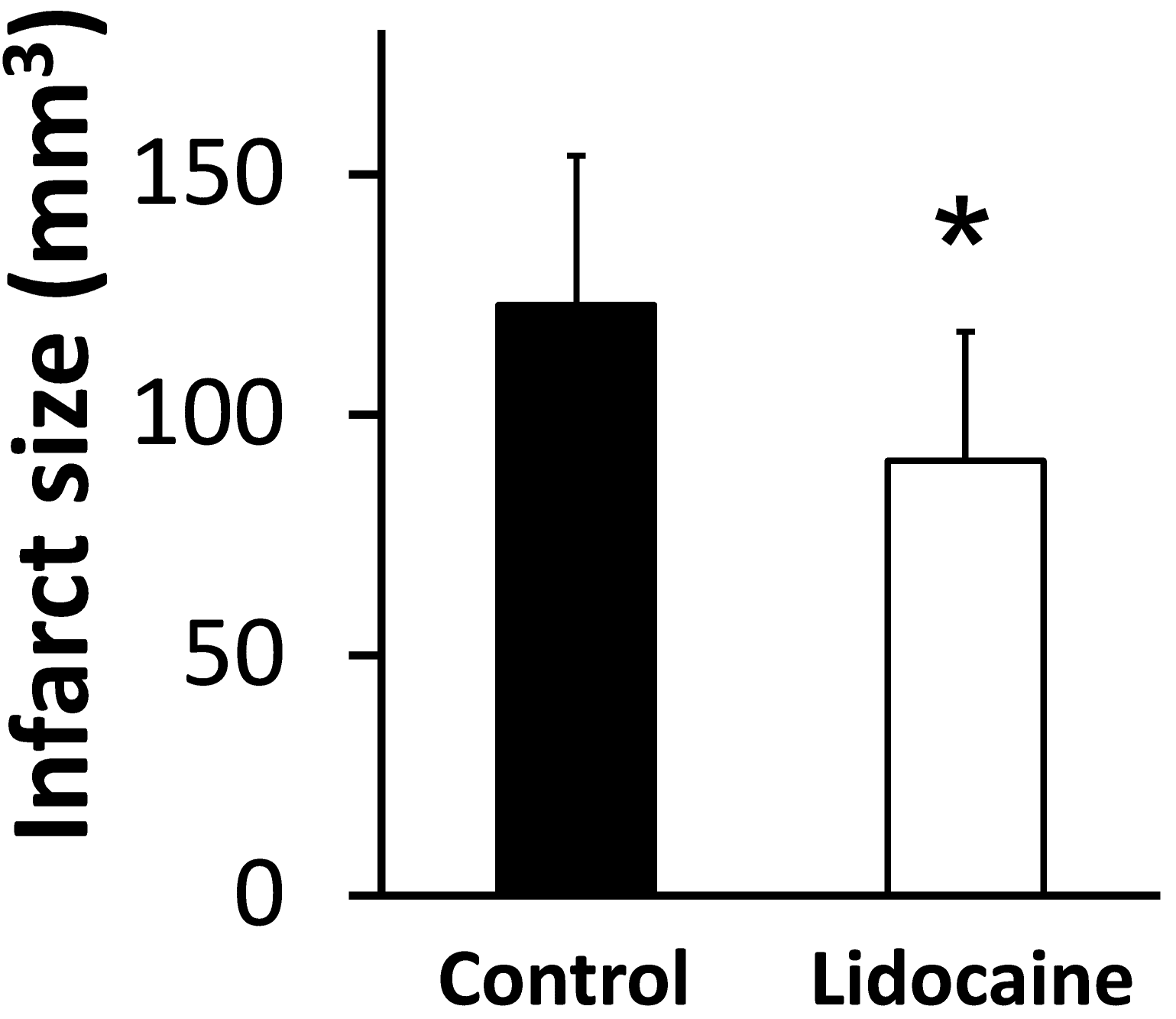
Infarct size (mm3)
150
100
50
0
*
Control
Lidocaine